Heliyon 8 (2022) e08994

Contents lists available at ScienceDirect

Heliyon

journal homepage: www.cell.com/heliyon

Research article

Immunological significance of alternative splicing prognostic signatures for bladder cancer

Xinyun Li [1], Lin Yang [1], Wei Huang, Bo Jia, Yu Lai [*]

School of Basic Medicine, Chengdu University of Traditional Chinese Medicine, Chengdu, China

ARTICLE INFO

Keywords:
Bladder cancer
Alternative splicing
Prognostic signature
Tumor immune microenvironment
Splicing factor

ABSTRACT

Background: Bladder cancer (BLCA) is the most common malignant tumor in the genitourinary system, and the complex tumor microenvironment (TME) of BLCA is the main factor in its difficult treatment. Accumulated evidence supports that alternative splicing (AS) events frequently occur in cancer and are closely related to the TME. Therefore, there is an urgent need to comprehensively analyze the prognostic value of AS events in BLCA.

Method: The clinical, transcriptome and AS data of BLCA were downloaded from the Cancer Genome Atlas database, and a Cox proportional hazard regression model and LASSO regression were used to establish a prognostic signature. Then, the prognostic value of the signature was verified by clinical survival status, clinicopathologic features, tumor immune microenvironment (TIME), and immune checkpoint. Next, we screened the AS-related genes with the largest expression differences between tumor and normal samples by gene differential expression analysis. Finally, the regulatory network of AS-splicing factors (SFs) was established to unravel the potential regulatory mechanism of AS events in BLCA.

Results: A BLCA prognostic signature related to seven AS events was constructed, and the prognostic value of the signature was also verified from multiple perspectives. Moreover, there was significant abnormal expression of *PTGER3*, a gene implicated in AS events, the expression of which was associated with the survival, clinicopathological features, TIME, and immunotherapy of BLCA, suggesting that it has potential clinical application value. Furthermore, the AS-SF regulatory network indicated that splicing factors (PRPF39, LUC7L, HSPA8 and DDX21) might be potential biomarkers of BLCA.

Conclusions: Our study revealed the potential role of AS events in the prognosis, TIME and immunotherapy of BLCA and yielded new insights into the molecular mechanisms of and personalized immunotherapy for BLCA.

1. Introduction

Bladder cancer (BLCA) is the most common malignant tumor of the urinary tract. According to the International Agency for Research on Cancer, in 2020, there were 573,278 new cases of BLCA and 212,536 new deaths worldwide, and the incidence rate in males was much higher than that in females [1]. Although smoking is the main risk factor [2], genetics [3], schistosomes [4] and aromatic amines [5] also have prominent effects on the occurrence of BLCA. The improvement of the BLCA treatment regimen can significantly prolong the overall survival (OS) of patients and reduce mortality. However, the therapeutic effects in advanced and metastatic BLCA are not ideal [6, 7, 8]. Therefore, we must urgently find new biomarkers and formulate new treatment schemes to help BLCA patients improve their OS.

The tumor microenvironment (TME) is composed of tumor cells, interstitial cells, microvessels, tissue fluid and infiltrating cells, which are vital to the occurrence, development and treatment of tumors [9, 10, 11]. As a popular research topic, the tumor immune microenvironment (TIME) has been found to play a variety of complex regulatory roles in BLCA and affect the prognosis of patients [12]. Fortunately, targeted immunotherapy, especially the use of immune checkpoint inhibitors (ICIs), such as PD-1, PD-L1 and CTLA4, has shown a positive effect in advanced BLCA [13, 14, 15]. However, due to the heterogeneity of BLCA, there are great differences in the efficacy of immunotherapy in patients [16]. Therefore, new molecular feature classification of BLCA patients and accurate prediction of the efficacy of immunotherapy will help to formulate personalized immunotherapy in the clinic.

* Corresponding author.
E-mail address: archimedean@rocketmail.com (Y. Lai).
[1] These authors contributed to the work equally.

https://doi.org/10.1016/j.heliyon.2022.e08994
Received 9 November 2021; Received in revised form 7 January 2022; Accepted 16 February 2022

Alternative splicing (AS) refers to the process of editing mRNA from the precursor to the mature mRNA. Since events increase genomic complexity and proteome diversity, they exist in almost 95% of the human genome [17]. AS events not only can regulate organ development and tissue identity acquisition, maintain tissue homeostasis and regulate cell function but also can have prominent effects on the occurrence and development of tumors [18,19]. In addition, tumor-specific mutations in splicing factors (SFs) are also risk factors for cancer development and maintenance [20]. The abnormal regulation of AS events can affect the TIME and change the survival time of tumor patients [21,22]. AS events have high potential application value in immunotherapy [23].

In recent years, multiple studies have found BLCA prognostic tools related to gene and immune cell infiltration [24,25], and previous studies have shown that AS events are associated with the prognosis of BLCA [26,27]. However, we still lack in-depth research on the mechanism of AS events in BLCA. With the development of technology and medicine, the evolution of high-throughput gene detection technology and large polycentric datasets of gene expression have made it possible for us to accurately identify pivotal molecular characteristics. To better serve the diagnosis and treatment of BLCA, immunotherapy programs should be formulated, and new anticancer drugs should be developed. We established a BLCA prognostic signature related to AS events, explored the relationship of AS events with the TIME, clinicopathologic features and immunotherapy, and identified new potential biomarkers related to AS events.

2. Materials and methods

2.1. Data acquisition and preprocessing

The main process of this study is shown in Figure 1 We downloaded the original transcriptome data and clinical information of BLCA patients from the Cancer Genome Atlas (TCGA) database (https://portal.gdc.cancer.gov/) and excluded samples with repetitive and missing survival information for follow-up analyses. The AS data corresponding to the samples came from TCGA SpliceSeq (https://bioinformatics.mdanderson.org/TCGASpliceSeq/PSIdownload.jsp). The percent spliced in (PSI) refers to the percentage of splicing, which is an indicator for quantifying the AS process. To ensure the reliability of subsequent analyses, we conducted a series of strict screenings on the samples (PSI values ≥ 0.75, average PSI value ≥ 0.05). The immunotherapy score file of the TCGA-BLCA cohort was downloaded from the Cancer Immune Atlas (TCIA) public database (https://www.tcia.at/home).

2.2. Process of AS event profiles

We classified the 7 subtypes (alternate acceptor site (AA), alternate donor site (AD), alternate promoter (AP), alternate terminator (AT), exon skip (ES), mutually exclusive exons (ME), and retained intron (RI)) of AS events included in the study and visualized the results of subtype interaction sets. This step used the UpSetR package in R software [28]. Next, we annotated the AS events included in this study. Combining the AS event gene, ID number and splicing type, for example, in "SUN1 | 78549 | ES", "SUN1″ is the name of the gene associated with the AS event, "78549″ is the splicing variant ID, and "ES" is the splicing type.

2.3. Identification of prognosis-related AS events and establishment of a risk assessment model

Univariate Cox analysis was used to investigate the relationship between AS events and OS in patients with BLCA, and AS events with $P < 0.05$ were selected as prognostic factors. A volcanic map and bubble maps were drawn to visualize AS events related to prognosis. The R packages survival, UpSetR and ggplot2 were used in the above operations. The selection operator LASSO Cox regression model with 10-fold cross-validation was used, and then candidate survival-related AS events were introduced into multivariate Cox regression analysis. Since the occurrence of each AS event was independent, we combined all of the AS PSI values with the corresponding regression coefficient (β) obtained by multivariate Cox analysis to calculate the risk score of each BLCA sample. The Eq. [1] is as follows:

$$Riskscore = \sum_{i=1}^{n} PSI_{AS_i} \times \beta_{ASi} \quad (1)$$

where n represents the total number of AS events, PSI_{ASi} represents the PSI value of one of the AS events, and β_{ASi} represents the corresponding regression coefficient.

After calculating the risk score of all samples, the patients with BLCA were divided into a high-risk group and a low-risk group with the median risk score as the cutoff point. The R packages used for model establishment included glmnet and survival.

2.4. Verification of the risk assessment model

We utilized Kaplan-Meier analysis to compare the OS between the high- and low-risk groups. The relationship between the risk score and survival status of each BLCA patient was also visualized. Univariate and multivariate Cox analyses were adopted to evaluate whether the model had independent prognostic value. Then, we used time-dependent receiver operating characteristic (ROC) curve analysis to evaluate the prognostic ability of the risk assessment model. In addition, Wilcoxon's signed rank test was used to calculate the differences in risk scores among groups with clinicopathologic features and evaluate the clinical application value of the model. To quantitatively predict the survival probability of each BLCA patient, we drew a nomogram according to the risk score and the clinical information from the TCGA database, including age, sex, tumor stage, grade, T category and N category. The accuracy of the nomogram was verified by calibration charts. When the slope of the calibration curve was closer to 1, the prediction ability of the nomogram was better. The R packages used in this section included survival, survminer, pheatmap, timeROC, limma, ggpubr and rms.

2.5. Correlation between the risk assessment model and TIME

First, the R package estimate was used to obtain the scores of stromal cells, immune cells and tumor purity in the TIME of BLCA patients, and a violin diagram was drawn to show the difference in results between the high- and low-risk groups. The TME score is the sum of the stromal score and immune score. Then, we calculated the proportion of 22 types of immune cells by CiberSort and drew a box graph and scatter diagrams using the R packets ggpubr, vioplot and ggExtra to illustrate the relationship between the risk score and infiltrating immune cells. Next, we used the R packet GSEAbase for single sample gene set enrichment analysis (ssGSEA) to investigate the expression differences in immune-related functional gene sets between risk score groups.

2.6. Correlation between the risk assessment model and immune checkpoint

The therapeutic effect of ICIs on tumors might be related to the expression level of genes related to immune checkpoints [29]. Therefore, we revealed the correlations among 6 critical genes related to immune checkpoints (PD-1, PD-L1, PDCD 1, HAVCR2, CTLA-4, IDO1) [30, 31, 32] and the risk score, setting the confidence level threshold to 0.95. For the immune checkpoint-related genes with significant expression differences between the high- and low-risk groups, we drew scatter plots to show the correlation results. We also investigated the differences in the expression of genes associated with 47 immune checkpoints and the differences in ICI treatment scores between different groups. The R packages limma, corrplot, ggpubr, ggExtra and ggplot2 were used in these steps.

2.7. Construction of an AS-SF regulatory network

Our study included 404 SF genes found by Seiler et al. [33] in somatic mutations (Supplementary Table 1). Combined with the SF RNA-seq data of BLCA patients downloaded from the TCGA database, the correlation between SFs and survival-related AS events was evaluated by univariate Cox analysis and detailed Spearman's correlation analysis. The filter criteria were set as follows: correlation coefficient >0.65 and P value <0.001. The drawing of the AS-SF regulatory network was completed by Cytoscape software, version 3.8.0.

2.8. Screening and verification of the prognostic gene related to AS events

We screened out prognostic genes related to AS events by gene differential expression analysis and set the reference value as log | FC | < 1.5 and P < 0.05. Using the median value of the gene expression level as the cutoff point, the samples were divided into high and low gene expression groups, and a Kaplan-Meier survival curve was drawn to compare the OS differences between the two groups. Wilcoxon's signed rank test was utilized to compare the gene expression differences in different clinicopathological characteristics and to evaluate the clinical application value of the gene. Next, we revealed the differences in immune checkpoint-related gene expression, TIME and immune infiltrating cells in the high and low gene expression groups. The expression level of the gene set in each sample was evaluated by ssGSEA, and the difference in immune gene set expression between the high and low expression groups of target genes was calculated. Finally, we analyzed the relationship of the gene expression level with immune infiltrating cells and immune checkpoint-related genes by Timer software, version 2.0.

2.9. Statistical analysis

Kaplan-Meier survival curves were used to observe all clinical survival differences in patients with BLCA. LASSO regression and Cox proportional hazard regression were adopted to construct a risk assessment model. The independent prognostic ability of the risk assessment model was verified by multivariate and univariate Cox regression. Wilcoxon's test and the Kruskal-Wallis test were used to compare the differences between two groups and three groups or more, respectively. The limma package in R was utilized for gene differential expression analysis. Pearson's chi-square test was used to analyze the differences in risk score, clinicopathologic features, immune checkpoints, TIME and infiltrating immune cells between groups. The ROC curves validated the predictive accuracy of the signature. For all of the hypothesis tests, a bilateral P < 0.05 was considered to be statistically significant; "*" indicates P < 0.05, "**" indicates P < 0.01, and "***" indicates P < 0.001. Except for the AS-SF regulatory network diagram, which was completed by Cytoscape software, version 3.8.0, all of the other statistical analyses and graphic drawings were performed using R software (version 4.0.4).

3. Results

3.1. Clinical information and AS event landscape of BLCA patients

A total of 412 valid clinical data samples were obtained from the TCGA database. The basic clinical information of the patients is shown in Table 1. We integrated the AS event data of BLCA patients. Then, 39,508 AS events were analyzed by gene intersection analysis of the 7 subtypes of AS events, and the results were visualized (Figure 2A). Among the types, exon skip (ES) is the most common type of AS, while mutually exclusive exons (ME) are the rarest.

3.2. Construction of the BLCA prognostic signature based on AS events

We identified 2,714 survival-related AS events through univariate Cox analysis (Figure 2B), of which ES and alternate promoter (AP) were the most common, accounting for 31.83% of survival-related AS events. We also described all of the survival-related AS events by volcanic mapping (Figure 1A) and seven different types of remarkable survival-related AS events by bubble mapping (Figure 1B-H).

Table 1. Baseline data of all BLCA patients.

Characteristic	Type	*n*	Proportion (%)
Age	≤65	162	39.32%
	>65	250	60.68%
Gender	female	108	26.21%
	male	304	73.79%
Grade	low	21	5.10%
	high	388	94.20%
	unknown	3	0.73%
Stage	Stage I–II	133	32.28%
	Stage III–IV	277	67.23%
	unknown	2	0.49%
T stage	T0–2	124	30.10%
	T3–4	255	61.89%
	unknown	33	8.10%
M stage	M0	196	47.57%
	M1	11	2.67%
	unknown	205	49.76%
N stage	N0–1	286	69.42%
	N2–3	84	20.39%
	unknown	42	10.19%

To obtain the AS events with the greatest prognostic value, we screened significant survival-related AS events using 10-fold cross-validation LASSO regression analysis and determined the optimal penalty parameter (Figure 2A-B), acquiring 11 survival-related AS events. On this basis, univariate Cox analysis was used to further screen the optimal survival-related AS events. Finally, we obtained 7 AS events to construct the BLCA prognostic signature (Supplementary Table 2).

3.3. Verification of the BLCA prognosis signature related to AS events

We constructed an AS event-related BLCA prognostic model based on multivariate Cox analysis, and calculated the risk score of each BLCA patient according to the model. Taking the median risk score as the cut-off point, the patients were divided into a high-risk group and a low-risk group (Supplementary Table 3). The results of Kaplan-Meier analysis showed that the OS of the low-risk group was prominently better than that of the high-risk group (P < 0.001; Figure 2C). We calculated the PSI value of the AS event for signature establishment and found that C19orf57|47943|ES, ACTG1|44120|RI, DYM|45472|ES and HPCAL1|52658|ES were highly expressed in low-risk patients, while ANK3|11845|AP, GRIK2|77096|AT and PTGER3|3415|AT were highly expressed in high-risk patients (Figure 2D). Percent spliced in (PSI) refers to the percentage of variable shear in genes, which is used to quantify the biological process of variable shear [34]. We visualized the risk score and clinical survival time of all samples. The results suggested that there was an obvious disadvantage in the clinical survival time of high-risk patients (Figure 2E-F). We also drew ROC curves of 1-, 2- and 3-year survival for the risk score, and their AUC values were ≥0.7 (Figure 2G), indicating that the risk assessment model has good predictive value. Moreover, univariate and multivariate Cox analyses confirmed that age, clinical stage and risk score were independent prognostic indicators (Figure 2H-I). Although the incidence of BLCA in males is higher than that in females, the sex of the patient is not an independent prognostic indicator. The reason for this result could be that the smoking rate in males is much higher than that in females [35].

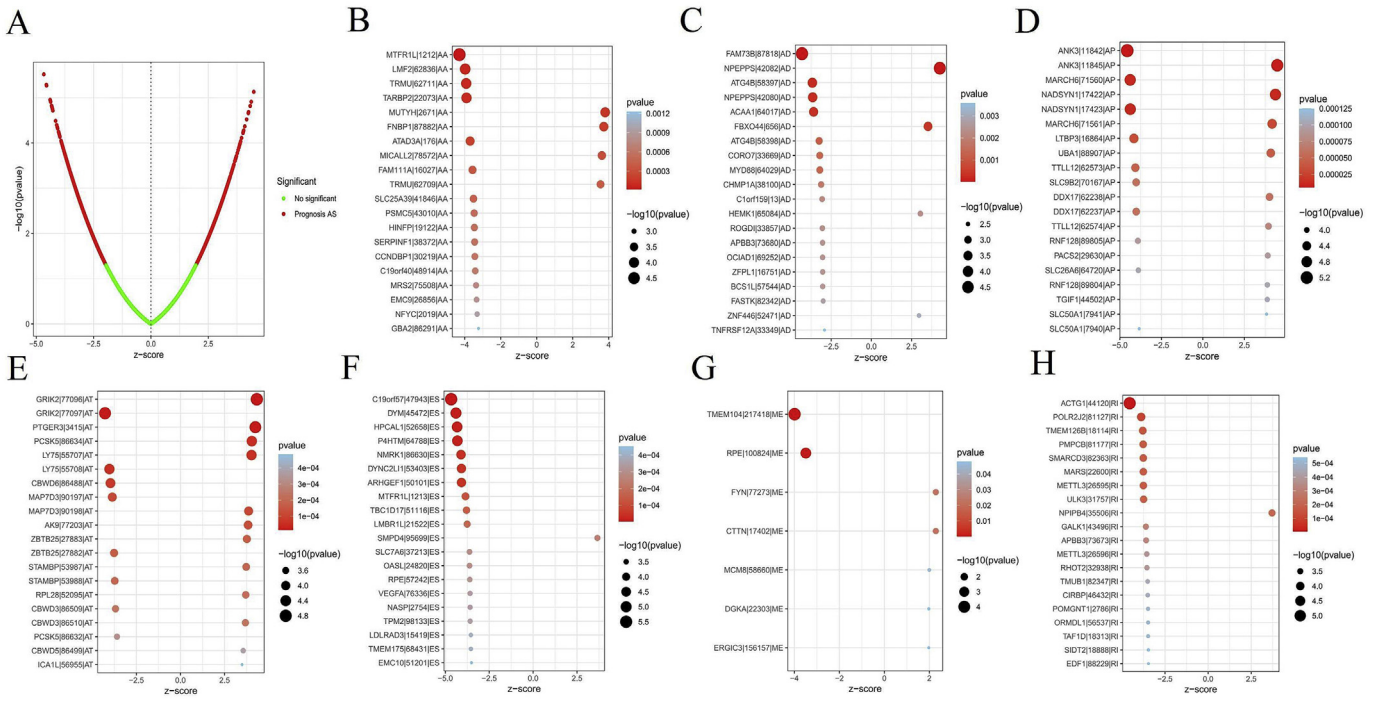

Figure 1. Survival related AS events. (A) The volcano map shows AS events related to survival. (B–H) The bubble charts display survival-related AS events in different types. (B) alternate acceptor site (AA); (C) alternate donor site (AD); (D) alternate promoter (AP); (E) alternate terminator (AT); (F) exon skip (ES); (G) mutually exclusive exons (ME); (H) retained intron (RI).

3.4. Correlations between risk score and clinicopathologic features and construction of a nomogram

To evaluate the clinical significance of the risk score, we revealed the differences in risk scores among subgroups with different clinicopathologic features. With the development of patient age, tumor grade and stage, the risk score showed an increasing trend. Among the scores, the risk scores of BLCA patients' age (Figure 3A), grade (Figure 3B), tumor stage (Figure 3C), M category (Figure 3D), T category (Figure S3A) and N category (Figure S3B) were significantly different. However, there was no significant correlation between sex (Figure S3C) and risk score. Next, we drew ROC curves of 1-, 2- and 3-year survival for the risk score and these clinical variables (Figure 3E-G), suggesting that the risk score is more sensitive and specific than traditional clinicopathologic features. On this basis, the points in the nomogram were used to scale the points produced by the variables to predict the 1-, 2- and 3-year OS of each BLCA patient (Figure 3H). In the nomogram, the risk score and each clinicopathological feature have corresponding scores at the top, and the total score obtained by adding all risk factor scores has corresponding 1-, 2- and 3-year survival rates at the bottom, which can be used to quantitatively predict the survival rate of each BLCA patient. In the 1-, 2- and 3-year OS calibration charts, the slopes of the correction curves were all close to 1, further confirming the good consistency between the predicted results and the clinical observations (Figure 3I-K). These results explained that the signature has predictive value in the clinic.

3.5. The risk assessment model and TIME

To research the role of the risk score in the TIME, we analyzed the relationship of the risk score with the immune score, the type and level of infiltrating immune cells, and the characteristics of ssGSEA. First, we used the estimate algorithm to score the TME of BLCA. The results indicated that there were significant differences in the TME score (Figure 4A), immune score (Figure 4B), stromal score (Figure 4C) and tumor purity (Figure 4D) between the high- and low-risk groups. Among the factors, the TME score, immune score and stromal score of patients in the high-risk group were higher, while tumor purity was lower. Subsequently, the results of the CiberSort algorithm suggested that there were striking, negative correlations between the risk score and naïve B cells, plasma cells, CD8 T cells, follicular helper T cells (Tfh) and regulatory T cells (Tregs) in the TME (Figure S4A-E). However, the risk score was positively correlated with M0 macrophages, M2 macrophages and resting memory CD4 T cells (Figure S4F-H). The box diagram indicated that plasma cells showed the greatest difference between patients in the high- and low-risk groups ($P < 0.001$). In addition, although there was no significant correlation between resting dendritic cells and the risk score, there was an obvious difference in resting dendritic cell infiltration levels between the high- and low-risk groups ($P < 0.05$; Figure 4E). These results suggested that the high TME score of patients in the high-risk and low-risk groups may be related to the participation of immune infiltrating cells in tumor activity, especially plasma cell infiltration, which was dominant in the low-risk group. However, contrary to our findings, Wei and his colleagues found that breast cancer patients with predominantly plasma cell infiltration had a significant survival disadvantage [36]. Subsequently, ssGSEA investigated the immune-related feature richness (Figure 4F) and gene expression differences (Figure 4G-H) of immune-related functional gene sets among groups. In the gene difference analysis of 29 immune-related function sets, there was significantly high expression of related genes in the high-risk group, which may indicate the immune activation state in the high-risk group. Enhanced humoral immunity and humoral immune-related factors can inhibit the tumor immune response, promote tumor angiogenesis and increase the risk of cancer [37]. The above results suggested that there was a connection between the risk score and TIME, providing a new way to study the immune regulation mechanism of BLCA.

3.6. Correlation between the risk score and immune checkpoint

To survey the relationship between the signature and immune checkpoints, we analyzed the correlations of the risk score with six critical immune checkpoint genes (CTLA-4, PDCD1, IDO1, CD274,

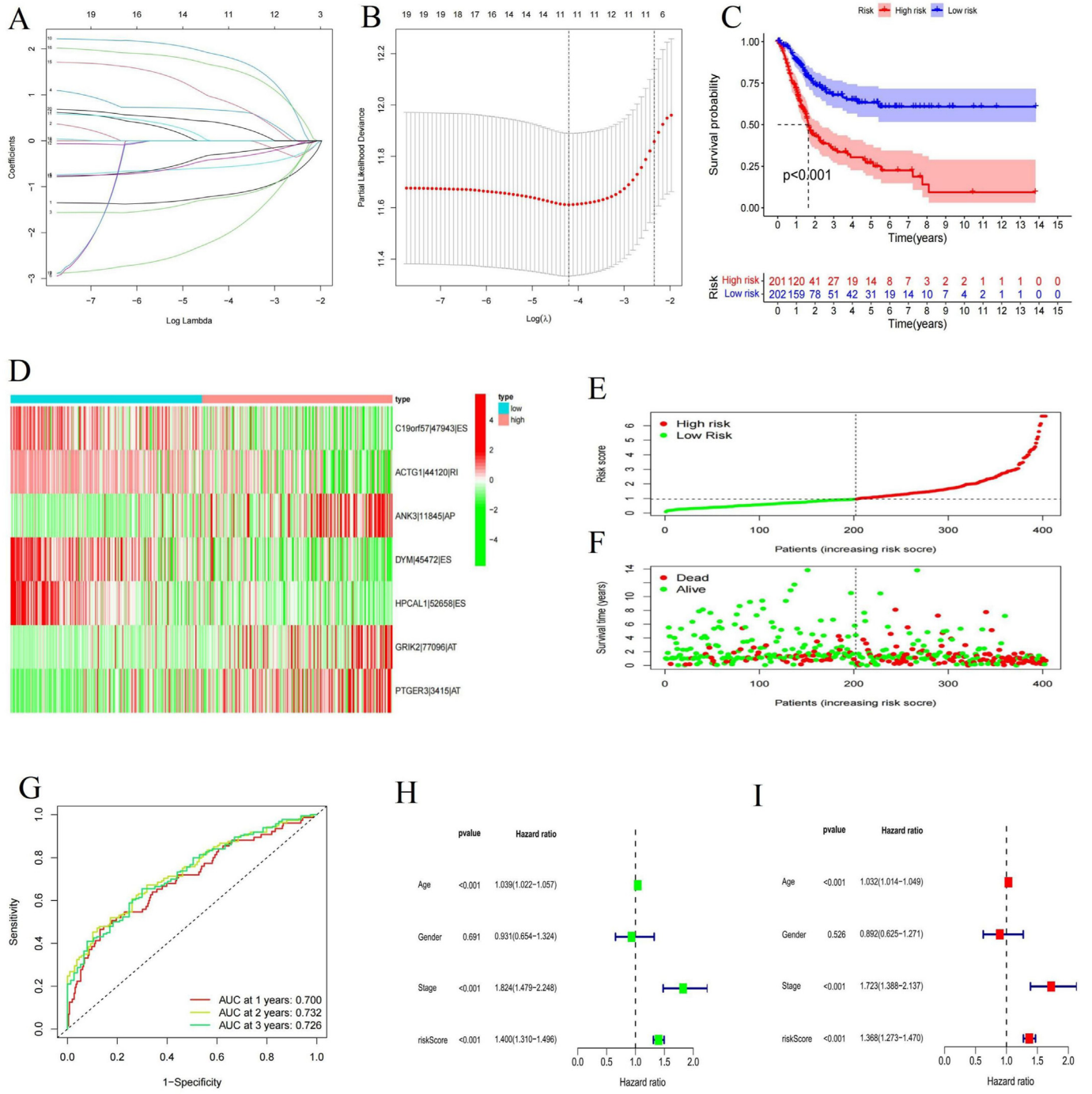

Figure 2. Construction of the prognostic signature of BLCA based on AS events. (A) The profile of AS events changing with the change in penalty coefficients in LASSO analysis. (B) Schematic diagram of calculating the optimal penalty parameter λ. The lower abscissa is the log (λ) value, and the ordinate is the degrees of freedom. Based on the λ value taken by the minimum criteria and 1-SE criteria, the corresponding number of AS events is 11. (C) The survival difference between the high- and low-risk groups was described by Kaplan-Meier survival curves. (D) Heatmap of the PSI of 7 AS events. Red indicates high expression, and green indicates low expression. (E) Risk score distribution of individual BLCA patients. (F) Risk scores and survival statuses of patients with BLCA. (G) The ROC curves of 1-, 2- and 3-year survival and the area under the curve (AUC) values were all ≥0.700. The closer the AUC value is to 1, the higher the accuracy of the signature. (H–I) The forest maps show the results of univariate Cox analysis (H) and multivariate Cox analysis (I).

HAVCR2 and PDCD1LG2). The results showed that the six genes were related to the risk score, and with the increase in the risk score, the expression of the six genes showed a significant upward trend: CTLA-4 (R = 0.28, p = 1.5e−08), PDCD1 (R = 0.27, p = 4.9e−08), IDO1 (R = 0.31, p = 4.4e−10), CD274 (R = 0.33, p = 9.8e−12), HAVCR2 (R = 0.41, p < 2.2e−16) and PDCD1LG2 (R = 0.48, p < 2.2e−16) (Figure 5A-G), suggesting that ICI therapy might be more advantageous in the high-risk group. The expression of 47 immune checkpoint-related genes displayed significant differences in different groups, except for TNFSF15, LGALS9, TNFRSF14, TNFRSF25 and TMIGD2, and the expression levels of other genes were higher in the high-risk group (Figure 5H). Immunotherapy scores indicated that patients in the low-risk group had higher immune

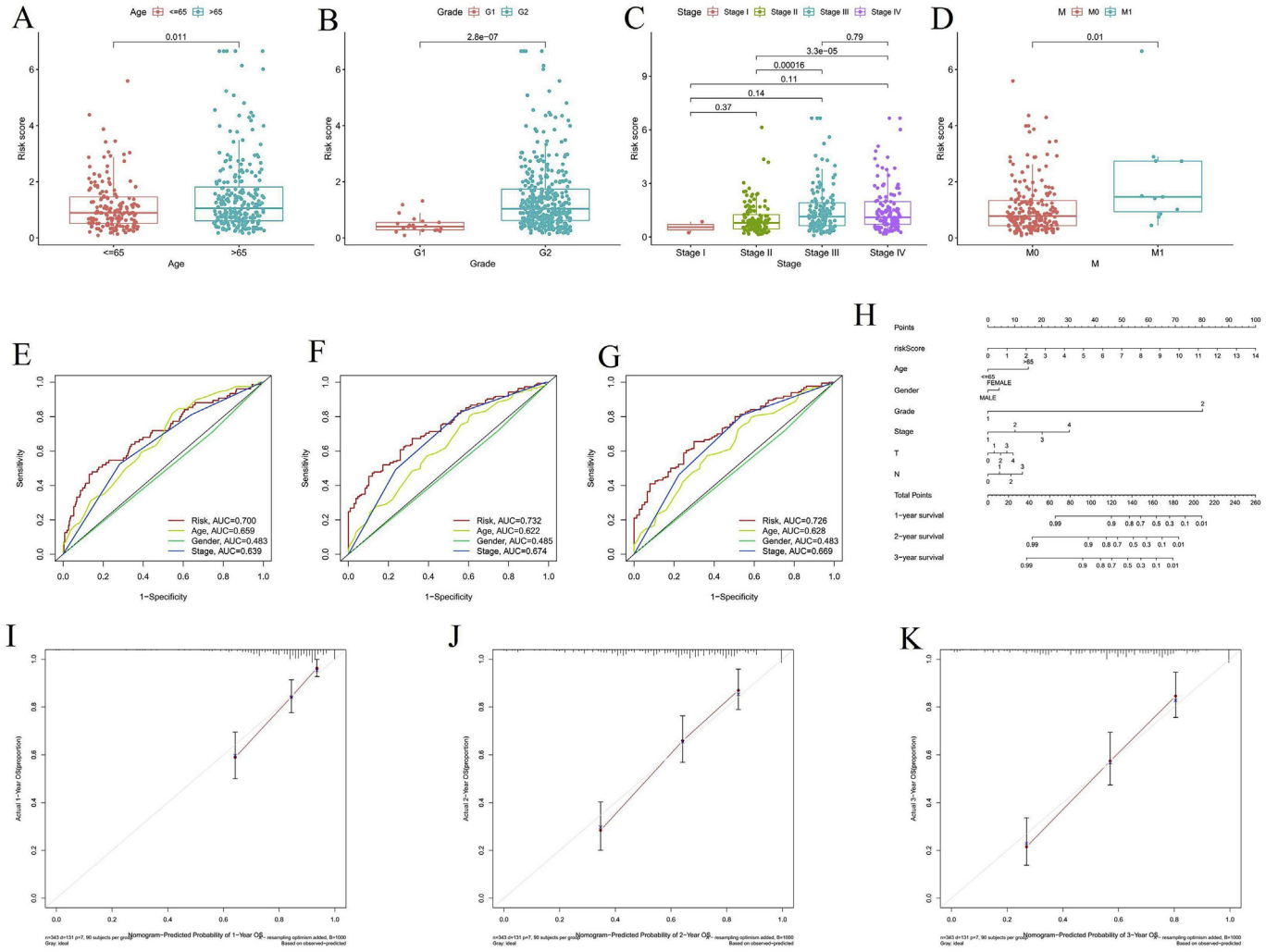

Figure 3. The relationship between the risk score and clinicopathological characteristics. (A–D) The differences in risk score among clinicopathological groups. (A) Age of patients; (B) grade; (C) tumor stage and (D) M category. (E–G) Comparing the ROC curves of the risk score and clinicopathological characteristics, the AUC values of the risk score were greater than those of the clinicopathological features. (E) 1-, (F) 2- and (G) 3-year survival. (H) A nomogram was compiled according to the risk score and clinicopathological characteristics to predict the OS of patients with BLCA. (I–K) The calibration charts showed that the predicted OS results were in good agreement with the actual clinical observations. (I) 1-, (J) 2- and (K) 3-year OS.

scores when treated without CTLA-4/PD-1 inhibitors (Figure 5I) and when only treated with CTLA-4 inhibitors (Figure 5J). When PD-1 inhibitors (Figure 5K) and CTLA-4/PD-1 (Figure 5L) inhibitors were used to treat BLCA patients, the difference in immunotherapy scores disappeared. Our results suggest that ICI therapy could have prominent effects on BLCA. Especially in high-risk patients, by blocking the immune escape of tumor cells, the effect of immunotherapy in the high-risk group could be basically the same as that in the low-risk group.

3.7. The AS-SF regulatory network

To investigate the mechanism between SFs and AS events, we built an AS-SF network diagram using Cytoscape software, version 3.8.0. Pearson's correlation tests were used to analyze the correlation between differentially expressed SFs and the PSI values of survival-related AS events. Through screening, we obtained 39 SFs, 38 upregulated AS events and 99 downregulated AS events. As shown in Figure 5, SFs had a positive correlation with most upregulated AS events and a negative correlation with most downregulated AS events. Moreover, we identified the top 5 nodes of connectivity (Table 2), which could be important factors involved in the abnormal regulation of AS in BLCA.

3.8. Verification of the prognosis of PTGER3 and its correlation with immune checkpoints

To further analyze the role of AS event-related genes in the prognosis and TIME of BLCA patients, we analyzed the differences among seven genes with AS events that constructed prognostic signatures. According to the gene expression of all samples in the TCGA-BLCA cohort, the gene expression differences between tumor tissues and normal tissues were analyzed, and the results are shown in Table 3. The results of gene differential expression analysis showed that the expression of *PTGER3* in normal tissues was much higher than that in tumor tissues ($P < 0.001$) (Figure 6A). Prostaglandin E receptor 3 (PTGER3), also known as EP3, is one of the four receptors of prostaglandin E2 (PGE2). It is a G-protein coupled receptor. Due to the unique structure of *PTGER3*, it can form at least 8 different splice isoforms, which are widely distributed in a variety of tissues and organs throughout the body and participate in numerous physiological and pathological activities, such as promoting uterine contraction during pregnancy, regulating bladder micturition and stimulating inflammatory swelling [38, 39, 40]. In addition, *PTGER3* mediates tumor lymphangiogenesis and the occurrence of many kinds of tumors, but the regulatory modes conflict with each other [41, 42, 43, 44, 45].

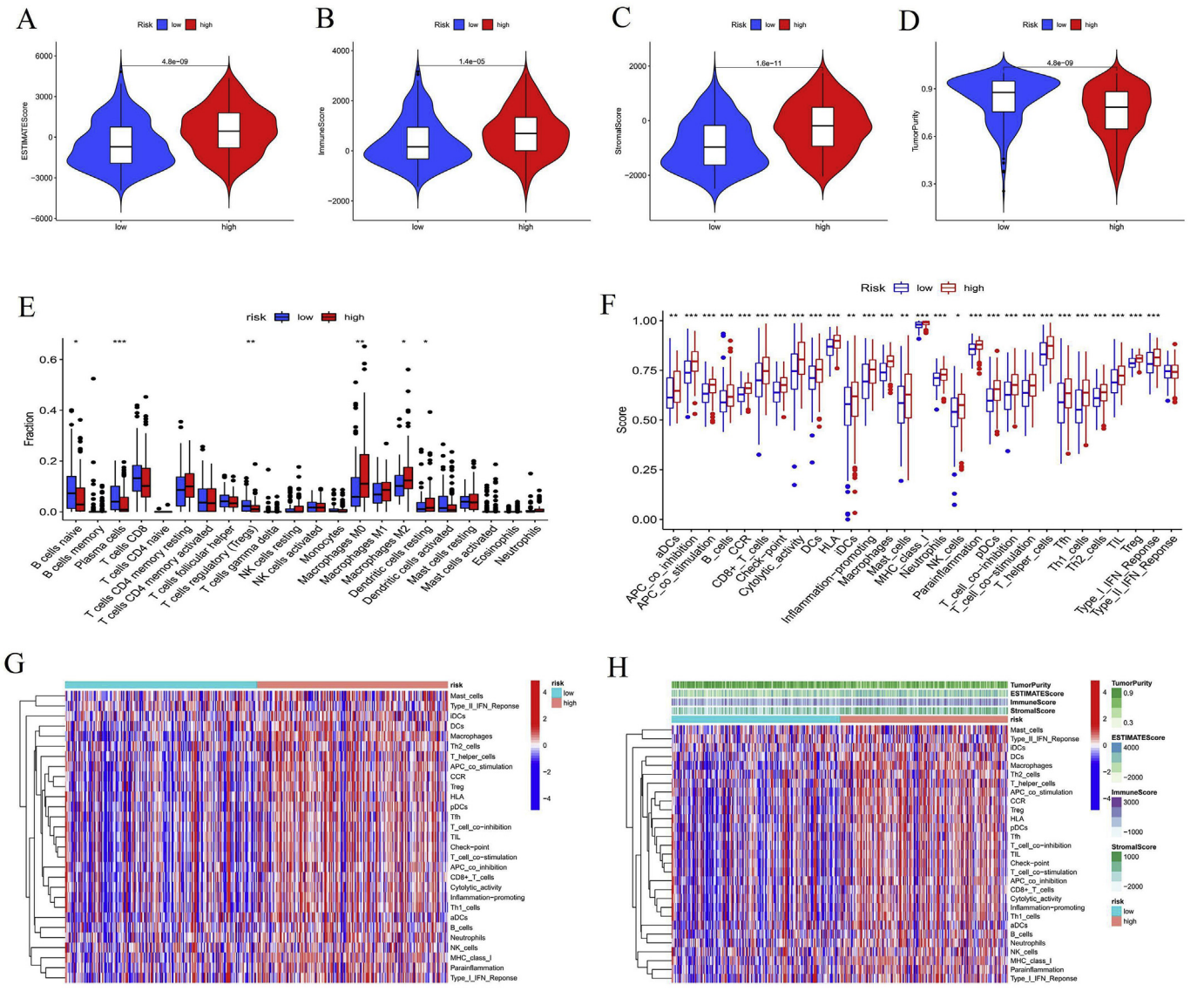

Figure 4. The risk score and TIME. (A–D) TME score (A), immune score (B), stromal score (C) and tumor purity (D) between the high- and low-risk groups. (E) The differences in the enrichment of immune infiltrating cells between groups. In the figure, * = $p < 0.05$, ** = $p < 0.01$, *** = $p < 0.001$.(F) Enrichment differences in immune function-related gene sets between groups. (G) The heatmap describes the differences in the expression of immune characteristic-related genes in different groups, with blue indicating downregulation and red indicating upregulation. (H) Heatmap of the TME score and immune gene expression of BLCA patients in different risk groups.

To study the role of *PTGER3* in BLCA, we further verified it. First, combined with the survival data of BLCA patients, Kaplan-Meier analysis was performed on patients in the high and low *PTGER3* expression groups. Patients in the low *PTGER3* group had longer OS ($P < 0.001$) (Figure 6B). Next, in the study of *PTGER3* expression levels in each group of clinicopathologic features, except for the age of the patients (Figure 6A), there were differences in *PTGER3* expression in other pathological subgroups (Figure 6B-G). Similar to the risk score of the clinicopathological subgroups, the expression of *PTGER3* increased with the age, tumor stage and grade of BLCA patients. Surprisingly, 47 immune checkpoint-related genes were significantly different between the different groups; among them, TNFRSF14 and TNFRSF25 were highly expressed in the low *PTGER3* group, and the other 45 genes were highly expressed in the high *PTGER3* group (Figure 6C). Finally, we also analyzed the relationship of *PTGER3* with tumor purity and key immune checkpoint-related genes in BLCA by TIMER2.0. The results suggested that the expression of *PTGER3* was negatively correlated with tumor purity ($R = -0.423$, $p = 2.05e{-}17$), and positively correlated with the immune checkpoint-related genes CD274 ($R = 0.071$, $p = 1.75e{-}01$), CTLA4 ($R = 0.174$, $p = 8.21e{-}04$), HAVCR2 ($R = 0.31$, $p = 1.27e{-}09$), PDCD1 ($R = 0.137$, $p = 8.5e{-}03$), PDCD1LG2 ($R = 0.284$, $p = 2.83e{-}08$), and IDO1 ($R = 0.024$, $p = 6.47e{-}01$) (Figure 6D-I). These findings jointly revealed that *PTGER3* was of great significance in the prognosis of BLCA, high PTGER3 expression indicated worse OS and lower tumor purity, and ICIs might be more effective in the treatment of patients with high *PTGER3*.

3.9. Correlation between PTGER3 and TIME

We conducted a series of analyses to clarify the role of *PTGER3* in the TIME of BLCA. The results of the estimation algorithm indicated that the low *PTGER3* group had lower TME scores, immune scores, and stromal scores and higher tumor purity (Figure 7A-D). Using the CIBERSORT algorithm, it was found that the expression level of *PTGER3* was positively correlated with naïve immune infiltrating B cells, M2 macrophages and resting mast cells and negatively correlated with activated dendritic

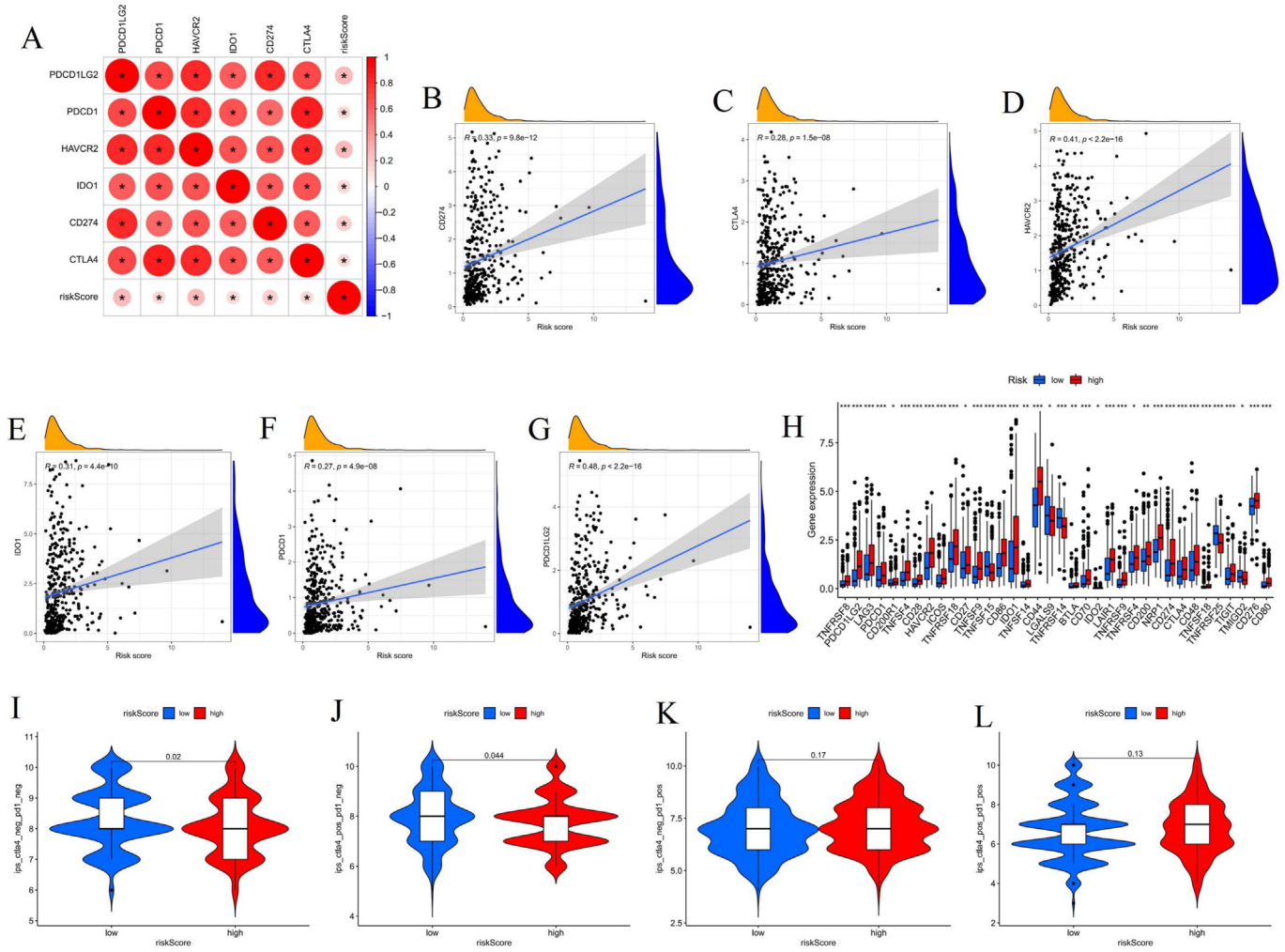

Figure 5. The association between the risk score and immune checkpoints. (A) The correlations of six critical immune checkpoint-related genes (CTLA-4, PDCD1, IDO1, CD274, HAVCR2 and PDCD1LG2) with the risk score; red indicates a positive correlation. * = p < 0.05, The larger the circle and the darker the color is, the stronger the correlation is, and the stronger correlation is shown by HAVCR2 and PDCD1LG2. (B–G) Scatter plots and straight regression lines show the correlation between the risk score and genes related to immune checkpoints. (B) CD274; (C) CTLA-4; (D) HAVCR2; (E) IDO1; (F) PDCD1 and (G) PDCD1LG2. (H) The expression differences in 47 immune checkpoint-related genes between different groups. (I–L) The different immunotherapy scores of the high- and low-risk groups were as follows: (I) no CTLA-4/PD-1 inhibitors, p = 0.02; (J) only CTLA-4 inhibitors, p = 0.044; (K) only PD-1 inhibitors, p = 0.17 and (L) CTLA-4/PD-1 inhibitors, p = 0.13. The upper and lower lines of the white rectangle in the middle of the violin diagram represent quartiles. The larger the area of the red and blue areas, the greater the probability of distribution near the ordinate values.

Table 2. Nodes with the top 5° in the AS-SF regulatory network.

Rank	Name	Degree
1	EIF3A	57
2	PRPF39	34
3	LUC7 L	27
4	HSPA8	11
5	DDX21	10

Table 3. Results of differential expression analysis of genes with AS events in normal and BLCA tumor tissues.

gene	conMean	treatMean	logFC	pValue
PTGER3	1.113564523	0.386840227	-0.726724296	3.40E-06

cells, activated mast cells, resting natural killer (NK) cells, activated memory CD4 T cells, CD8 T cells and Tfh cells (Figure 7A-I). There were differences in 7 types of infiltrating immune cells between the high and low *PTGER3* groups (Figure 7E). ssGSEA pointed out that, except for the gene sets of interdigitating dendritic cells (iDCs) and NK cells, there were distinct differences in the expression of the other 27 immune-related gene sets between the high and low *PTGER3* groups (Figure 7F). Higher expressions of DCs, B cells, checkpoint, macrophages and other immune-related genes were found in the high *PTGER3* group, suggesting that there may be more active immune activity in BLCA tumors with high *PTGER3* expression. TIMER 2.0 analysis suggested that there was a significant relationship between the expression of *PTGER3* and the infiltration levels of multiple immune cells (Figure 7G). Through CVN analysis in TIMER 2.0, we also found that, in the immune infiltrating cells of BLCA, CD4+ T cells and myeloid dendritic cells showed copy number deletions, while B cells and macrophages displayed copy number acquisitions (Figure 8A-D).

4. Discussion

BLCA is the most common urologic malignancy with high tumor heterogeneity [46,47]. With changes in the immune status of cancer treatment becoming increasingly prominent, bacille Calmette Guerin bladder instillation, ICIs and other immunotherapies have achieved

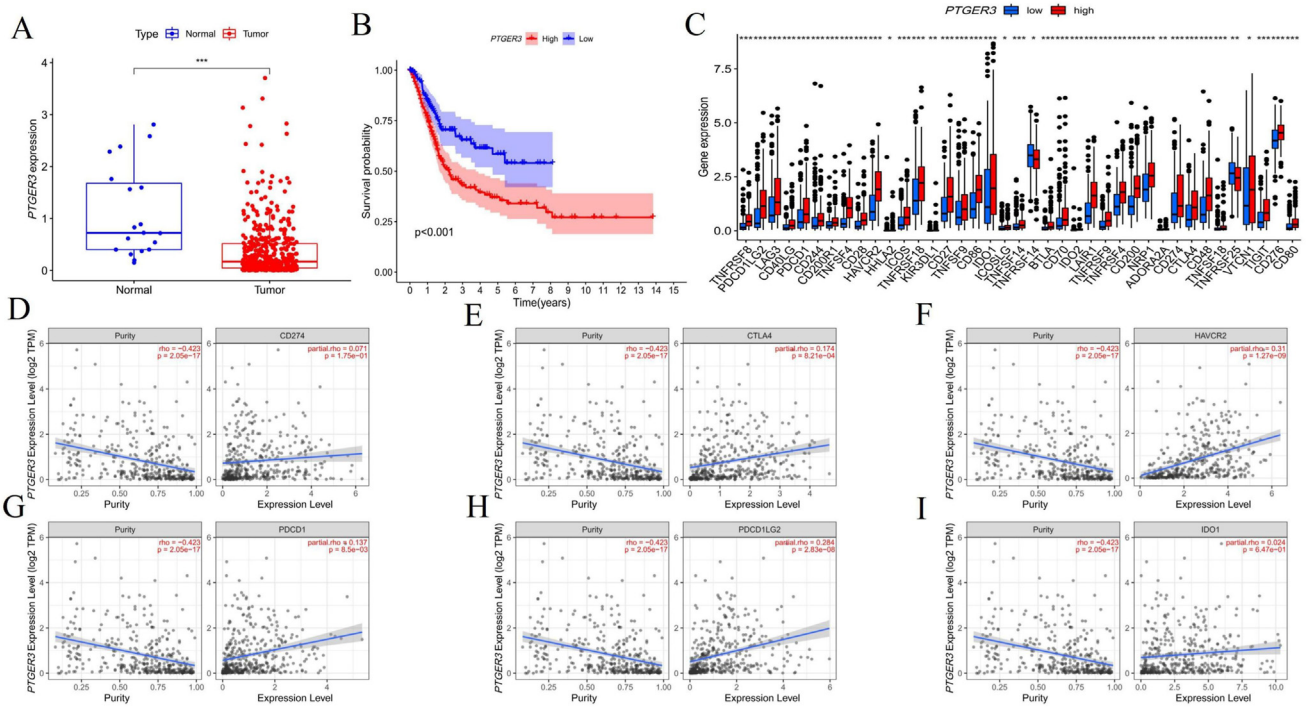

Figure 6. Prognostic role of *PTGER3* in BLCA and its relationship with immune checkpoints. (A) The difference in *PTGER3* expression between normal tissue and tumor tissue, $p < 0.001$. (B) Kaplan–Meier analysis showed the difference in survival between the high and low *PTGER3* groups, $p < 0.001$. (C) The expression differences in 47 immune checkpoint-related genes between groups, and the differences in all genes were statistically significant, $p < 0.05$. (D–G) Scatter plots and linear regression lines show the correlation of the expression level of *PTGER3* with tumor purity and six key immune checkpoint genes. (D) CD274; (E) CTLA4; (F) HAVCR2; (G) PDCD1; (H) PDCD1LG2; (I) IDO1.

certain curative effects in BLCA. However, immunotherapy for BLCA is also highly individual specific, and many BLCA patients do not respond to immunotherapy [48,49]. Therefore, we must urgently establish a signature that can effectively predict the prognosis of BLCA and the effect of immunotherapy to help clinical treatment and prolong the OS of patients. AS has been providing to play an important role in human physiological and pathological activities [50]. Especially in the process of tumor occurrence and development, AS has definite diagnostic value and the possibility of providing potential biomarkers for predicting the prognosis of tumors [51]. However, we still lack research on AS events in the field of TIME and immunotherapy.

We established a BLCA prognostic signature based on 7 AS events, in which C19orf57|47943|ES, ACTG1|44120|RI, DYM|45472|ES and HPCAL1|52658|ES were protective AS events, and ANK3|11845|AP, GRIK2|77096|AT and PTGER3|3415|AT were dangerous AS events. *ACTG1* is overexpressed in uterine cancer cells, and shows an inhibitory response to immunotherapy [52]. Aerobic glycolysis inhibits the proliferation of hepatocellular carcinoma (HCC) cells by downregulating *ACTG1*, and a high level of *ACTG1* is significantly related to advanced hepatoma [53]. *HPCAL1* increases the proliferation and growth of glioblastoma by activating the Wnt/β-catenin pathway [54]. Yeon et al. [55] found that 13.9% of colorectal cancers (CRCs) in 124 patients had *ANK3* gene frameshift mutations and intratumoral heterogeneity, and low expression of *ANK3* could inhibit detachment-induced apoptosis and promote CRC cell survival. The overexpression of *GRIK2* is associated with the phenotype of less aggressive sarcoma and the senescence of ovarian cancer cells [56,57]. Interestingly, overexpression of *GRIK2* increases the invasive ability and tumorigenicity of urothelial carcinoma (UC) stem cells, which is related to poor prognosis in UC [58]. Although it has been found that the abnormal expression of *ACTG1*, *HPCAL1*, *ANK3* and *GRIK2* is related to tumors, these 7 AS events have not been studied by scholars, and they could be potential biomarkers of BLCA.

The estimation algorithm and ssGSEA indicated that the high-risk group had higher immune scores and higher expression levels of immune characteristic-related genes. It is suggested that BLCA patients in the high-risk group might have strong immune activity and exert antitumor effects through an immune effect mechanism. The infiltration levels of naïve B cells, plasma cells, CD8 T cells, Tfhs and Tregs in the TME in the high-risk group were lower than those in the low-risk group, but the infiltration levels of M0 macrophages, M2 macrophages and resting memory CD4 T cells were higher. High levels of CD8 T cells have been found to be associated with better prognosis of BLCA and younger women with breast cancer [59,60]. In patients with CRC, the high expression of Tfh-related genes suggests a better prognosis. However, due to PD-1/PD-L1-mediated inhibition, the ability of Tfhs to stimulate CD8+ T cells and produce IL-21 is weakened in patients with advanced CRC [61]. Treg infiltration is associated with poor prognosis of BLCA [62, 63]. M0 macrophages are related to poor prognosis of HCC [64]. M2 macrophages are involved in tumor microangiogenesis in BLCA and are related to tumor stage and invasiveness [65]. Because of the diversity and complexity of immune infiltrating cells in the TME, the results of multiple types of immune infiltrating cell analysis will be more valuable than single-type immune cell analysis.

The immunotherapy score survey revealed that, with the use of CTLA-4/PD-1 inhibitors, the immunotherapy difference between the high- and low-risk groups decreased. This outcome could be related to the higher expression of immune checkpoint-related genes in the high-risk group. Durvalumab, a PD-L1 inhibitor, showed safe clinical significance in a phase 1/2 multicenter BLCA clinical trial, in which the objective response rate (ORR) of PD-L1-positive patients was 46.4%, and the ORR of PD-L1-negative patients was 0% [66]. In a multicenter, phase 1/2 CheckMate032 trial, the PD-1 inhibitor nivolumab showed an ORR of 24.4% in patients with refractory metastatic UC [14]. Powles et al. [67] found that the PD-L1 inhibitor MPDL3280A could help to treat metastatic UC, and the ORR of PD-L1-positive patients was higher, precisely because ICIs

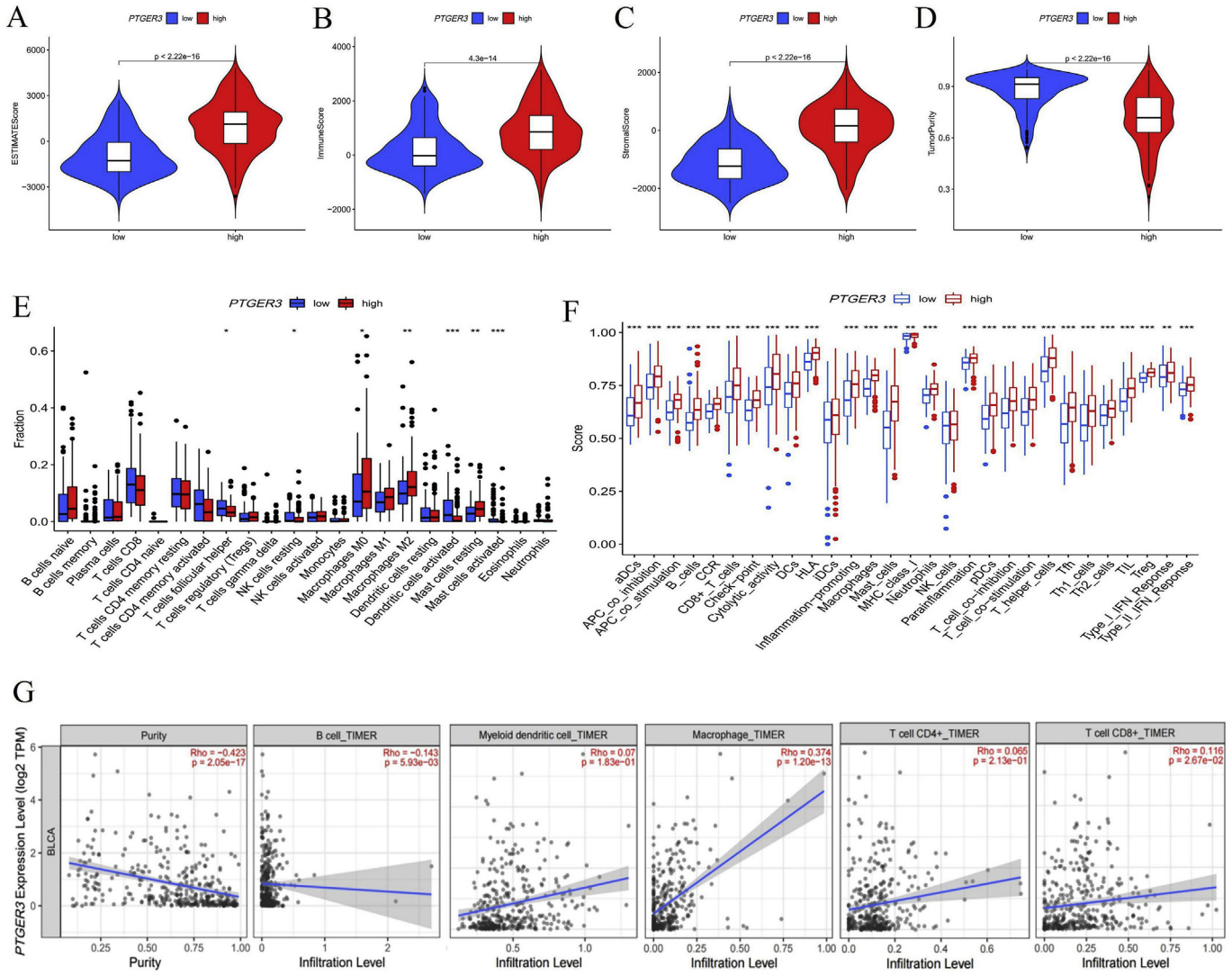

Figure 7. *PTGER3* and TIME. (A–D) The differences in TME score (A), immune score (B), stromal score (C) and tumor purity (D) between the high and low *PTGER3* groups. (E) The degree of difference in immune cell infiltration between groups. (F) Differences in immune characteristic enrichment between groups, ** = $p < 0.01$ and *** = $p < 0.001$. (G) Scatter plots and linear regression lines depict the correlation between *PTGER3* expression levels and different types of immune cell infiltration.

have clinical application value in BLCA, and the immunotherapeutic effect of patients varies greatly. In this study, we analyzed the correlation between the risk score and immune checkpoints. Although these findings suggested that patients with BLCA in the high-risk group might have a better therapeutic effect on ICIs, the detailed molecular mechanisms should be further elucidated. Nevertheless, the signature could be used as a new predictive tool for formulating BLCA immunotherapy strategies.

Gene differential expression analysis indicated that there were significant differences in *PTGER3* between BLCA tissues and normal tissues. Our study found that the OS of patients in the high *PTGER3* group was shorter, but the expression of immune checkpoint-related genes, the enrichment of immune characteristic-related genes and the number of immune infiltrating cells in the high *PTGER3* group were higher than those in the low *PTGER3* group, suggesting that the high *PTGER3* group might correspond to the state of immune activation, but the antitumor effect of immune cells could be blocked by the immune checkpoint. A previous study showed that *PTGER3* is overexpressed in tumors and adjacent tissues of CRC [68]. The high expression of *PTGER3* is also related to the shortening of OS in patients with ovarian cancer, but silencing prostaglandin E2 receptor EP3 (PTGER3) could improve cisplatin resistance through the RAS-MAPK/ERK-ET-ELK1 axis [69,70]. Our study found for the first time that abnormal expression of *PTGER3* is related to BLCA, revealing that *PTGER3* could be a potential biomarker for the prognosis of BLCA and a potential target for immunotherapy.

SFs play a carcinogenic or inhibitory role by participating in abnormal AS events in BLCA [71,72]. Consequently, we constructed an AS-SF regulatory network of BLCA to visually demonstrate the abnormal AS regulatory mechanism of BLCA. The five most important SF centers were eIF3a, PRPF39, LUC7L, HSPA8 and DDX21, which could have significant effects on the occurrence and development of BLCA. Downregulation of eIF3a can decrease the movement, proliferation and growth rate of mouse BLCA cells, and high expression of eIF3a can shorten the OS of low-grade BLCA patients [73]. However, PRPF39, LUC7L, HSPA8 and DDX21 are the first SFs that might be involved in the development of BLCA. The AS-SF regulatory network provides a basis for further study of the mechanism of AS events in BLCA and the development of new antineoplastic drugs.

5. Conclusions

We analyzed the regulatory role of AS events and constructed a signature that can predict the prognosis of BLCA. In addition, the verification

results of clinical survival status, clinicopathologic features, ROC curves and nomograms showed that our signature has reliable predictive value. The correlation analysis of the risk score with TIME and immune checkpoints also suggested predictive value in immunotherapy. This work emphasized that the *PTGER3* gene and splicing factors PRPF39, LUC7L, HSPA8 and DDX21 might be potential biomarkers of BLCA. In summary, AS events provide a new perspective on the prognosis of BLCA and the formulation of new immunotherapy strategies. The AS-SF regulatory network supplies a basis for research on the regulatory mechanism of AS in BLCA. However, further experiments and clinical explorations remain necessary to verify the clinical value of the signature and *PTGER3* in BLCA.

Declarations

Author contribution statement

Xinyun Li: Performed the experiments; Analyzed and interpreted the data; Wrote the paper.

Lin Yang: Contributed reagents, materials, analysis tools or data; Wrote the paper.

Yu Lai; Bo Jia; Wei Huang: Conceived and designed the experiments; Analyzed and interpreted the data.

Funding statement

This work was supported by the Xinglin Scholar Research Promotion Project of Chengdu University of TCM (grant number XSGG2020001).

Data availability statement

Data included in article/supplementary material/referenced in article.

Declaration of interests statement

The authors declare no conflict of interest.

Additional information

Supplementary content related to this article has been published online at https://doi.org/10.1016/j.heliyon.2022.e08994.

Acknowledgements

Not applicable.

References

[1] H. Sung, J. Ferlay, R.L. Siegel, et al., Global cancer statistics 2020: GLOBOCAN estimates of incidence and mortality worldwide for 36 cancers in 185 countries, CA A Cancer J. Clin. 71 (2021) 209–249.
[2] M.G. Cumberbatch, M. Rota, J.W.F. Catto, C.L. Vecchia, The role of tobacco smoke in bladder and kidney carcinogenesis: a comparison of exposures and meta-analysis of incidence and mortality risks, Eur. Urol. 70 (2016) 458–466.
[3] O. Antonova, D. Toncheva, E. Grigorov, Bladder cancer risk from the perspective of genetic polymorphisms in the carcinogen metabolizing enzymes, J. Buon 20 (2015) 1397–1406.
[4] D.M. Parkin, The global burden of urinary bladder cancer, Scand. J. Urol. Nephrol. Suppl. (2008) 12–20.
[5] V.J. Cogliano, R. Baan, K. Straif, et al., Preventable exposures associated with human cancers, J. Natl. Cancer Inst. 103 (2011) 1827–1839.
[6] H.E. Karim-Kos, Ed Vries, I. Soerjomataram, V. Lemmens, S. Siesling, J.W.W. Coebergh, Recent trends of cancer in Europe: a combined approach of incidence, survival and mortality for 17 cancer sites since the 1990s, Eur. J. Cancer 44 (2008) 1345–1389.
[7] Maase Hvd, S.W. Hansen, J.T. Roberts, et al., Gemcitabine and cisplatin versus methotrexate, vinblastine, doxorubicin, and cisplatin in advanced or metastatic bladder cancer: results of a large, randomized, multinational, multicenter, phase III study, J. Clin. Oncol. 18 (2000) 3068–3077.
[8] J.T. Roberts, Maase Hvd, L. Sengeløv, et al., Long-term survival results of a randomized trial comparing gemcitabine/cisplatin and methotrexate/vinblastine/ doxorubicin/cisplatin in patients with locally advanced and metastatic bladder cancer, Ann. Oncol. 17 (2006) v118–v122.
[9] I.J. Fidler, The pathogenesis of cancer metastasis: the 'seed and soil' hypothesis revisited, Nat. Rev. Cancer 3 (2003) 453–458.
[10] C.E. Weber, P.C. Kuo, The tumor microenvironment, Surg. Oncol. 21 (2011) 172–177.
[11] Nv Dijk, S.A. Funt, C.U. Blank, Powles, J.E. Rosenberg, Heijden MSvd, The cancer immunogram as a framework for personalized immunotherapy in urothelial cancer, Eur. Urol. 75 (2019) 435–444.
[12] M.L. Eich, A. Chaux, G. Guner, et al., Tumor immune microenvironment in non-muscle-invasive urothelial carcinoma of the bladder, Hum. Pathol. 89 (2019) 24–32.
[13] D.P. Petrylak, T. Powles, J. Bellmunt, et al., Atezolizumab (MPDL3280A) monotherapy for patients with metastatic urothelial cancer: long-term outcomes from a phase 1 study, JAMA Oncol. 4 (2018) 537–544.
[14] P. Sharma, M.K. Callahan, P. Bono, et al., Nivolumab monotherapy in recurrent metastatic urothelial carcinoma (CheckMate 032): a multicentre, open-label, two-stage, multi-arm, phase 1/2 trial, Lancet Oncol. 17 (2016) 1590–1598.
[15] J. Bellmunt, R. Wit, D.J. Vaughn, et al., Pembrolizumab as second-line therapy for advanced urothelial carcinoma, N. Engl. J. Med. 376 (2017) 1015–1026.
[16] M. Eckstein, R.M. Wirtz, C. Pfannstil, et al., A multicenter round robin test of PD-L1 expression assessment in urothelial bladder cancer by immunohistochemistry and RT-qPCR with emphasis on prognosis prediction after radical cystectomy, Oncotarget 9 (2018) 15001–15014.
[17] Q. Pan, O. Shai, L.J. Lee, B.J. Frey, B.J. Blencowe, Deep surveying of alternative splicing complexity in the human transcriptome by high-throughput sequencing, Nat. Genet. 40 (2009) 1413–1415.
[18] F.E. Baralle, J. Giudice, Alternative splicing as a regulator of development and tissue identity, Mol. Cell. Biol. 18 (2017) 437–451.
[19] D. Pradella, C. Naro, C. Sette, C. Ghigna, EMT and stemness: flexible processes tuned by alternative splicing in development and cancer progression, Mol. Cancer 16 (2017) 8, 8.
[20] E.E. Marabti, I. Younis, The cancer spliceome: reprograming of alternative splicing in cancer, Front. Mol. Biosci. 5 (2018) 80.
[21] E.K. Kim, S.O. Yoon, W.Y. Jung, et al., Implications of NOVA1 suppression within the microenvironment of gastric cancer: association with immune cell dysregulation, Gastric Cancer 20 (2017) 438–447.
[22] Z.-X. Li, Z.-Q. Zheng, Z.-H. Wei, et al., Comprehensive characterization of the alternative splicing landscape in head and neck squamous cell carcinoma reveals novel events associated with tumorigenesis and the immune microenvironment, Theranostics 9 (2019) 7648–7665.
[23] L. Frankiw, D. Baltimore, G. Li, Alternative mRNA splicing in cancer immunotherapy, Immunology 19 (2019) 675–687.
[24] A. Ariafarab, Y. Vahidic, M. Fakhimic, A. Asadollahpourb, N. Erfanicd, Z. Faghihc, Prognostic significance of CD4-positive regulatory T cells in tumor draining lymph nodes from patients with bladder cancer, Heliyon 6 (2020), e05556.
[25] Z.H. Chen, G.J. Liu, A. Hossain, et al., A co-expression network for differentially expressed genes in bladder cancer and a risk score model for predicting survival, Hereditas 156 (2019) 24.
[26] S. Han, D. Kim, M. Shivakumar, The effects of alternative splicing on miRNA binding sites in bladder cancer, PLoS One (2018), e0190708.
[27] Z. Guo, H. Zhu, W. Xu, et al., Alternative splicing related genetic variants contribute to bladder cancer risk, Mol. Carcinog. 59 (2020) 923–929.
[28] J.R. Conway, A. Lex, N. Gehlenborg, UpSetR: an R package for the visualization of intersecting sets and their properties, Bioinformatics 33 (2017) 2938–2940.
[29] A. Goodman, S.P. Patel, R. Kurzrock, PD-1-PD-L1 immune-checkpoint blockade in B-cell lymphomas, Nat. Rev. Clin. Oncol. 14 (2017) 203–220.
[30] J.E. Kim, M.A. Patel, A. Mangraviti, et al., Combination therapy with anti-PD-1, anti-TIM-3, and focal radiation results in regression of murine gliomas, Clin. Cancer Res. 24 (2018) 124–136.
[31] L. Zhai, E. Ladomersky, A. Lenzen, et al., Ido1 in cancer: a Gemini of immune checkpoints Cell, Mol. Immunol. 15 (2018) 447–457.
[32] M. Nishino, N.H. Ramaiya, H. Hatabu, F.S. Hodi, Monitoring immune-checkpoint blockade: response evaluation and biomarker development, Nat. Rev. Clin. Oncol. 14 (2017) 655–668.
[33] M. Seiler, S. Peng, A.A. Agrawal, et al., Somatic mutational landscape of splicing factor genes and their functional consequences across 33 cancer types, Cell Rep. 23 (2018).
[34] D. Zhang, Y. Duan, J. Cun, Q. Yang, Identification of prognostic alternative splicing signature in breast carcinoma, Front. Genet. 10 (2019) 278.
[35] S. Amiri, Worldwide prevalence of smoking in immigration: a global systematic review and meta-analysis, J. Addict. Dis. 38 (2020) 1–13.
[36] H.Y. Wei, P.F. Fu, M.Y. Yao, Y.M. Chen, L.L. Du, Breast cancer stem cells phenotype and plasma cell-predominant breast cancer independently indicate poor survival, Pathol. Res. Pract. 212 (2016) 294–301.
[37] T.T. Tan, L.M. Coussens, Humoral immunity, inflammation and cancer, Curr. Opin. Immunol. 19 (2007) 209–216.
[38] M. Kotani, I. Tanaka, Y. Ogawa, et al., Structural organization of the human prostaglandin EP3 receptor subtype Gene (PTGER3) Genomics 40, 1997, pp. 425–434.
[39] K. Morimoto, N. Shirata, Y. Taketomi, et al., Prostaglandin E2–EP3 signaling induces inflammatory swelling by mast cell activation, J. Immunol. 192 (2014) 1130–1137.
[40] X. Su, E.S.R. Lashinger, L.A. Leon, et al., An excitatory role for peripheral EP3 receptors in bladder afferent function, Am. J. Physiol. Ren. Physiol. 295 (2008) F585–F594.

[41] S. Narumiya, H. Amano, T. Suzuki, et al., Host prostaglandin EP3 receptor signaling relevant to tumor-associated lymphangiogenesis, Biomed. Pharmacother. 64 (2010) 101–106.
[42] Lvd Emde, D. Goltz, S. Latz, et al., Prostaglandin receptors EP1-4 as a potential marker for clinical outcome in urothelial bladder cancer, Am. J. Cancer Res. 4 (2014) 952–962.
[43] T. Yano, G. Zissel, J. Muller-Qernheim, S.J. Shin, H. Satoh, T. Ichikawa, Prostaglandin E2 reinforces the activation of Ras signal pathway in lung adenocarcinoma cells via EP3, FEBS (Fed. Eur. Biochem. Soc.) Lett. 518 (2002) 154–158.
[44] Y. YS, M. Takahashi, T. Kitamura, et al., Downregulation of prostaglandin E receptor subtype EP3 during colon cancer development, Gut 53 (2004) 1151–1158.
[45] Y. Ye, L. Peng, A. Vattai, et al., Prostaglandin E2 receptor 3 (EP3) signaling promotes migration of cervical cancer via urokinase-type plasminogen activator receptor (uPAR), J. Cancer Res. Clin. Oncol. 146 (2020) 2189–2203.
[46] J.I. Warrick, G. Sjodahl, M. Kaag, et al., Intratumoral heterogeneity of bladder cancer by molecular subtypes and histologic variants, Eur. Urol. 75 (2019) 18–22.
[47] Y.W. Zhang, C.R. Zhu, M.P. Curado, T.Z. Zheng, P. Boyle, Changing patterns of bladder cancer in the USA: evidence of heterogeneous disease, BJU Int. 109 (2012) 52–56.
[48] A.V. Balar, M.D. Galsky, J.E. Rosenberg, et al., Atezolizumab as first-line treatment in cisplatin-ineligible patients with locally advanced and metastatic urothelial carcinoma: a single-arm, multicentre, phase 2 trial, Lancet 389 (2017) 67–76.
[49] C. Pettenati, M.A. Ingersoll, Mechanisms of BCG immunotherapy and its outlook for bladder cancer, Nat. Rev. Urol. 15 (2018) 615–625.
[50] T.W. Nilsen, B.R. Graveley, Expansion of the eukaryotic proteome by alternative splicing, Nature 463 (2010) 457–463.
[51] B.M.N. Brinkman, Splice variants as cancer biomarkers Clinical Biochemistry 37, 2004, pp. 584–594.
[52] C. Richter, D. Mayhew, J.P. Rennhack, et al., Genomic amplification and functional dependency of the gamma actin gene *ACTG1* in uterine cancer, Int. J. Mol. Sci. 21 (2020) E8690.
[53] Y.C. Yan, H. Xu, L.S. Zhang, et al., RRAD suppresses the Warburg effect by downregulating *ACTG1* in hepatocellular carcinoma, OncoTargets Ther. 12 (2019) 1691–1703.
[54] D.M. Zhang, X.D. Liu, X.B. Xu, et al., HPCAL1 promotes glioblastoma proliferation via activation of Wnt/β-catenin signalling pathway, J. Cell Mol. Med. 23 (2019) 3108–3117.
[55] S.Y. Yeon, Y.S. Jo, E.J. Choi, M.S. Kim, N.J. Yoo, S.H. Lee, Frameshift mutations in repeat sequences of *ANK3, HACD4, TCP10L, TP53BP1, MFN1, LCMT2, RNMT, TRMT6, METTL8* and *METTL16* genes in colon cancers, Pathol. Oncol. Res. 24 (2018) 617–622.
[56] J.G. Mayers, N. Gokgoz, J.S. Wunder, I.L. Andrulis, Investigation of the effects of alterations in the glutamate receptor, *GRIK2*, on osteosarcoma tumorigenesis, Clin. Cancer Res. 24 (2018).
[57] V.K. Zhawar, R.P. Kandpal, R.S. Athwal, Isoforms of ionotropic glutamate receptor *GRIK2* induce senescence of carcinoma cells, CANCER GENOMICS PROTEOMICS 16 (2019) 59–64.
[58] R. Inoue, Y. Hirohashi, H. Kitamura, et al., *GRIK2* has a role in the maintenance of urothelial carcinoma stem-like cells, and its expression is associated with poorer prognosis, Oncotarget 8 (2017) 28826–28839.
[59] T. Horn, J. Laus, A. Seitz, et al., The prognostic effect of tumour-infiltrating lymphocytic subpopulations in bladder cancer, World J. Urol. 34 (2016) 181–187.
[60] Y.W. Jin, P. Hu, Tumor-infiltrating CD8 T cells predict clinical breast cancer outcomes in young women, Cancers 12 (2020) 1076.
[61] W.W. Shi, L. Dong, Q. Sun, H. Ding, J. Meng, G.H. Dai, Follicular helper T cells promote the effector functions of CD8+ T cells via the provision of IL-21, which is downregulated due to PD-1/PD-L1-mediated suppression in colorectal cancer, Exp. Cell Res. 372 (2018) 35–42.
[62] Y.N. Liu, H. Zhang, L. Zhang, et al., Sphingosine 1 phosphate receptor-1 (S1P1) promotes tumor-associated regulatory T cell expansion: leading to poor survival in bladder cancer, Cell Death Dis. 10 (2019) 50.
[63] S. Maeda, K. Murakami, A. Inoue, T. Yonezawa, N. Matsuki, CCR4 blockade depletes regulatory T cells and prolongs survival in a canine model of bladder cancer, Cancer Immunol. Res. 7 (2019) 1175–1187.
[64] M. Farha, N.K. Jairath, T.S. Lawrence, I.E. Naqa, Characterization of the tumor immune microenvironment identifies M0 macrophage-enriched cluster as a poor prognostic factor in hepatocellular carcinoma, JCO Clin. Cancer Info. 4 (2020) 1002–1013.
[65] H. Takeuchi, M. Tanaka, A. Tanaka, A. Tsunemi, H. Yamamoto, Predominance of M2-polarized macrophages in bladder cancer affects angiogenesis, tumor grade and invasiveness, Oncol. Lett. 11 (2016) 3403–3408.
[66] C. Massard, M.S. Gordon, S. Sharma, et al., Safety and efficacy of durvalumab (MEDI4736), an anti-programmed cell death ligand-1 immune checkpoint inhibitor, in patients with advanced urothelial bladder cancer, J. Clin. Oncol. 34 (2016) 3119–3125.
[67] T. Powles, J.P. Eder, G.D. Fine, et al., MPDL3280A (anti-PD-L1) treatment leads to clinical activity in metastatic bladder cancer, Nature 515 (2014) 558–562.
[68] I. Cebola, J. Custodio, M. Munoz, et al., Epigenetics override pro-inflammatory PTGS transcriptomic signature towards selective hyperactivation of PGE2 in colorectal cancer, Clin. Epigenet. 7 (2015) 74.
[69] C. Rodriguez-Aguayo, E. Bayraktar, C. Ivan, et al., PTGER3 induces ovary tumorigenesis and confers resistance to cisplatin therapy through up-regulation Ras-MAPK/Erk-ETS1-ELK1/CFTR1 axis, EBioMedicine 40 (2019) 290–304.
[70] E. Bayraktar, C. Rodriguez-Aguayo, Z. Siddik, G. Lopez-Berestein, Delivery of 2F-PS2 PTGER3 siRNA-DOPC enhances anti-tumoral activity in cisplatin resistant ovarian cancer model, Cancer Res. 77 (2017) 2066.
[71] S.D. Stasi, P. Bielli, V. Panzeri, et al., The splicing factor PTBP1 promotes expression of oncogenic splice variants and predicts poor prognosis in patients with non-muscle invasive bladder cancer European Urology Supplements 18, 2019, e3356.
[72] H. Yoshino, H. Enokida, T. Chiyomaru, Tumor suppressive microRNA-1 mediated novel apoptosis pathways through direct inhibition of splicing factor serine/arginine-rich 9 (SRSF9/SRp30c) in bladder cancer Biochemical and Biophysical Research Communications 417, 2012, pp. 588–593.
[73] R. Spilka, C. Ernst, H. Bergler, et al., eIF3a is over-expressed in urinary bladder cancer and influences its phenotype independent of translation initiation, Cell. Oncol. 37 (2014) 253–267.